

This particular example also illustrates another point made by Wolf<sup>5</sup> and Van Vleck<sup>6</sup>—that the anisotropy in the exchange field may not be the same as that in the  $g$  tensor. If we diagonalize the matrix of

$$\mathcal{H}_{\text{Zeeman}} = -g_J \beta H (J_z \cos \theta - J_y \sin \theta) \quad (16)$$

in our Kramers basis we find that the eigenvalues are

$$E_{1,2} = \pm \frac{1}{2} g_J \beta H (A \cos^2 \theta + B \sin^2 \theta)^{1/2}, \quad (17)$$

where  $A$  and  $B$  are functions of the single-ion spin-orbit and crystal-field parameters. We see that there is no  $\sin \theta \cos \theta$  term. Therefore, the  $g$  tensor defined by

$$\mathcal{H}_{\text{eff}} = \beta \vec{H} \cdot \vec{g} \cdot \vec{S} \quad (18)$$

will not have antisymmetric components.

A number of recent papers<sup>6-8</sup> have pointed out that assuming an isotropic exchange between two electrons may lead to an exchange interaction which is anisotropic if expressed in the effective spin of a Kramers doublet or in the total spin of a multielectron atom. This same result appears in the present example. Suppose that instead of the Coulomb interaction of Eq. (3) we have assumed the isotropic exchange operator

$$\mathcal{H}_{f-d} = J \vec{S}_f \cdot \vec{S}_d \quad (19)$$

Again assuming basis states of Eq. (5) we obtain a splitting of the Kramers doublet given

$$E_{1,2} = \pm \frac{1}{2} J S_d \{ [\langle \varphi_1 | \varphi_1 \rangle - \langle \varphi_2 | \varphi_2 \rangle]^2 \cos^2 \theta + [\langle \varphi_1 | \varphi_1^* \rangle + \langle \varphi_2 | \varphi_2^* \rangle]^2 \sin^2 \theta \}^{1/2}. \quad (20)$$

We see that the splitting is indeed anisotropic but that it fails to contain the  $\sin \theta \cos \theta$  terms characteristic of antisymmetric exchange. Even if we allow a different isotropic exchange constant for each  $|l, l_z\rangle$  state of the  $4f$  electron, we do not obtain an antisymmetric splitting. We conclude, therefore, that the isotropic exchange operator  $\vec{S}_1 \cdot \vec{S}_2$  does not lead directly to antisymmetric exchange, and that one must have recourse to the true Coulombic exchange interaction of Eq. (3) if one is to obtain a correct picture of the origin of antisymmetric exchange.

\*Work supported in part by the Advanced Research Projects Agency through the Center for Materials Research at Stanford University, and in part by the National Science Foundation under Grant No. GK-1646.

<sup>1</sup>I. Dzyaloshinsky, J. Phys. Chem. Solids 4, 241 (1958).

<sup>2</sup>T. Moriya, Phys. Rev. 120, 91 (1960).

<sup>3</sup>M. T. Hutchings, C. G. Windsor, and W. P. Wolf, Phys. Rev. 148, 444 (1966); Z. Sroubek, R. Zdansky, and M. Vichr, Phys. Letters 21, 264 (1964).

<sup>4</sup>T. J. Beaulieu, Stanford University Microwave Laboratory Report No. 1530, 1967 (unpublished).

<sup>5</sup>W. P. Wolf, Proc. Phys. Soc. (London) 74, 665 (1959).

<sup>6</sup>J. H. Van Vleck, Rev. Univ. Nac. Tucumán, Ser. A 14, 189 (1962).

<sup>7</sup>P. M. Levy, Phys. Rev. 135, A155 (1964).

<sup>8</sup>R. J. Elliott, in Proceedings of the International Congress on Magnetism, Boston, Massachusetts, September, 1967 (to be published).

## EVIDENCE FOR ELECTRON-TO-PHONON INTERACTION IN InSb

D. H. Dickey\* and D. M. Larsen

Lincoln Laboratory, † Massachusetts Institute of Technology, Lexington, Massachusetts

(Received 9 November 1967)

We have observed anomalies in the spectrum of shallow donor impurities in a magnetic field in InSb. Our data show complicated polaron anomalies which indicate that an electron-TO-phonon interaction exists in InSb and is of strength comparable with the electron-LO-phonon interaction in this material.

Because strong Reststrahl absorption obscures observations in the region where polaron pin-

ning occurs,<sup>1,2</sup> the pinning phenomenon has, until the present, not been observed in intraband magnetoabsorption. Pinning has been reported only in interband experiments<sup>3,4</sup> where a detailed interpretation of the phenomenon is made difficult by complex exciton and valence band structure. The intraband experiment reported here lends itself to much more straightforward interpretation than do the interband

observations and circumvents the Reststrahl problem inherent in cyclotron resonance measurements. This latter advantage is achieved by utilizing combined resonance,<sup>5</sup> in which the electron in absorbing a photon simultaneously flips its spin and changes its Landau quantum number.

Figure 1 indicates schematically the levels important to our experiment and shows why pinning effects, if present, can be observed in combined resonance although not in cyclotron resonance. Full arrows designate free-carrier and impurity combined resonance transitions; dotted arrows connect levels expected to be strongly coupled by electron-optical-phonon interaction when the applied magnetic field,  $H$ , approaches the critical region ( $\sim 35$ - $38$  kOe).

In Fig. 1 and the following we use the notation<sup>6</sup>  $(n\uparrow)$ ,  $(n\downarrow)$ =Landau levels with spin up, down ( $n=0$  or  $1$ );  $(0\uparrow)_I$ ,  $(0\downarrow)_I$ =impurity ground-state levels for spin up, down;  $(1\uparrow)_I$ =lowest lying impurity level with orbital angular momentum  $\hbar$  along the magnetic field and spin down; and  $E_{n\uparrow}$ ,  $E_{n\downarrow}$ =energy of spin-up Landau level, impurity level.

The critical field  $H_c$  near which we expect to see polaron anomalies in the energy of  $(1\uparrow)_I$  due to the interaction of electrons and optical phonons (LO or TO) of energy  $\hbar\omega_0$  is defined by

$$E_{I1\downarrow}(H_c) - E_{I0\downarrow}(H_c) = \hbar\omega_0. \quad (1)$$

At field  $H_c$  the energy of the impurity com-

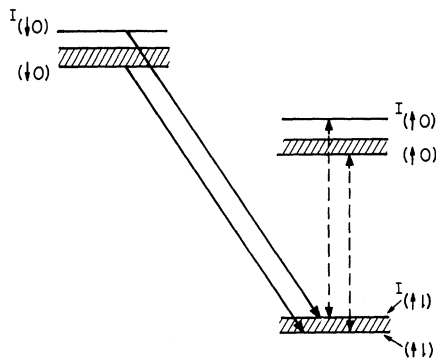


FIG. 1. Schematic diagram of relevant InSb conduction-band energy levels in a magnetic field. The shaded areas represent closely spaced impurity levels associated with the labeled Landau levels. Although the  $(1\uparrow)_I$  level probably does not lie exactly at the bottom of the impurity continuum associated with  $(1\uparrow)$ , we have drawn it there for clarity.

bined resonance transition is

$$E_{I1\downarrow}(H_c) - E_{I0\downarrow}(H_c) = \hbar\omega_0 + S_I. \quad (2)$$

$H_c \cong 35.5$  kOe for TO phonons and  $\sim 38$  kOe for LO phonons,  $S_I$  is the spin splitting of the  $n=0$  impurity ground-state levels at  $H_c$ , and we use the values<sup>7</sup>

$$\begin{aligned} \hbar\omega_{TO} &= 22.9 \pm 0.4 \text{ meV}, \\ \hbar\omega_{LO} &= 24.45 \pm 0.25 \text{ meV}. \end{aligned} \quad (3)$$

Taking  $S_I$  to range near 10 meV for our critical fields, we conclude that the incident energy required for exciting the impurity combined resonance transition when  $H \sim H_c$  is roughly 10 meV above  $\hbar\omega_{TO}$ . This is sufficiently far from the Reststrahl to allow us to study impurity combined resonance transitions for  $H$  near  $H_c$  in our samples of  $\sim 2.5$  mm thickness. Similar considerations apply to the free-carrier combined resonance transition.

Experiment.—Polarized radiation incident upon the sample with electric vector along the applied magnetic field was swept in frequency at fixed  $H$ , and the transmitted energy  $T(H, \nu)$  recorded. Minima found in the ratio  $T(H, \nu)/T(0, \nu)$  plotted as a function of photon energy  $h\nu$  are recorded in Fig. 2 for each field studied. Data were taken with a far-infrared spectrometer at both "low" and "high" temperature in order to distinguish impurity from free-carrier transitions. Our samples, mounted with the  $\langle 110 \rangle$  direction parallel to the magnetic field, had carrier concentrations in the range  $(1.2-1.6) \times 10^{15} \text{ cm}^{-3}$  and mobilities near  $3 \times 10^5 \text{ cm}^2/\text{V sec}$ .

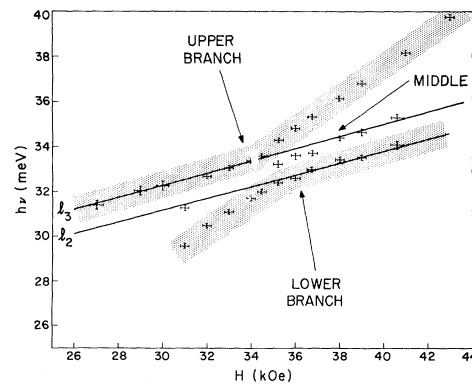


FIG. 2. Photon energy  $\hbar\nu$  at transmission minimum versus magnetic field  $H$  near the critical-field region in InSb. Lines  $l_2$  and  $l_3$  are fitted to the data as described in the text.

Turning to the data of Fig. 2, we find that the impurity spectrum shown there divides itself into three branches which are denoted "lower," "middle," and "upper."

At low fields ( $H < 35$  kG) the strongest absorption is on the lower branch; at high fields, on the upper branch. The middle branch is always weakly absorbing. The lower branch which pins to (approaches asymptotically)  $l_2$  from below decreases in absorption strength with increasing  $H$  for  $H$  greater than the appropriate critical field. On the other hand, the low-field absorption along  $l_3$  decreases with decreasing field.

Rigid-lattice band theory, well understood for the conduction band of InSb, predicts nonlinear behavior of the cyclotron-resonance absorption energy plotted against magnetic field. However, these effects are far too small to account for the bending of the lower branch. We can gain no clue to the origin of the rich structure shown in Fig. 2 from the band calculations.

Of crucial importance to the interpretation of the data of Fig. 2 are the positions and slope of lines  $l_2$  and  $l_3$ . To obtain these lines we measured the high-temperature cyclotron-resonance energy,  $E_{1\downarrow} - E_{0\uparrow}$ , and the free-carrier combined resonance energy,  $E_{1\downarrow} - E_{0\uparrow}$ , for fields below 32 kOe. By taking the difference of these measured energies we obtain experimentally the spin splitting of the  $n=0$  free-carrier levels,  $E_{0\downarrow} - E_{0\uparrow}$ , as a function of field. Finding  $E_{0\downarrow} - E_{0\uparrow}$  to be linear in field up to 32 kOe within experimental error we linearly extrapolated the spin splitting to fields as high as 42 kOe. Denoting the extrapolated spin splitting by  $S(H)$ , we attempted to fit the high-field part of the lower branch by  $S(H) + C_{LB}$  (which is  $l_2$  in Fig. 2) and the low-field part of the upper branch by  $S(H) + C_{UB}$  (which is  $l_3$ ) where the  $C$ 's are constants. We find an excellent fit if we take

$$C_{LB} = 23.0 \text{ meV and } C_{UB} = 24.1 \text{ meV.}$$

The agreement between  $C_{LB}$  and  $\hbar\omega_{TO}$  and between  $C_{UB}$  and  $\hbar\omega_{LO}$  from (3) is reasonably good.

Calculations of  $E_{I0\uparrow}(H)$  and  $E_{I0\downarrow}(H)$  by the method of Larsen<sup>8</sup> indicate that to an excellent approximation

$$E_{I0\downarrow}(H) - E_{I0\uparrow}(H) \equiv S_I(H) = S(H).$$

Inspection of Fig. 1 and the identification  $C_{LB}$

$= \hbar\omega_{TO}$  and  $C_{UB} = \hbar\omega_{LO}$  leads us to conclude therefore that  $E_{I1\downarrow}$  pins to  $E_{I0\downarrow} + \hbar\omega_{LO}$  on the middle and upper branches and to  $E_{I0\downarrow} + \hbar\omega_{TO}$  on the lower and possibly the middle branch.

This behavior can be understood at least qualitatively from a Fröhlich-type polaron theory in which we add to the standard Fröhlich Hamiltonian a TO-phonon energy term and an electron-TO-phonon interaction of the form

$$\sum_{\vec{k}, \mu} \hbar\omega_{TO} C_{\vec{k}\mu}^\dagger C_{\vec{k}\mu} + \sum_{\vec{k}, \mu} f_{\mu}(\vec{k}) (e^{-i\vec{k}\cdot\vec{r}} C_{\vec{k}\mu}^\dagger + e^{i\vec{k}\cdot\vec{r}} C_{\vec{k}\mu}), \quad (4)$$

where  $C_{\vec{k}\mu}^\dagger$  creates a TO phonon of wave vector  $\vec{k}$  and polarization  $\mu$  ( $\mu = 1, 2$ ). Such a theory in the weak-coupling limit gives essentially

$$\mathcal{E}_I = \hbar\omega_I - \frac{(M_{TO} \hbar\omega_{TO})^2}{\hbar\omega_{TO} - \mathcal{E}_I} - \frac{(M_{LO} \hbar\omega_{LO})^2}{\hbar\omega_{LO} - \mathcal{E}_I}, \quad (5)$$

where  $\mathcal{E}_I$  is the observed impurity transition energy,  $\hbar\omega_I$  is the impurity transition energy that would be observed in rigid lattice, and  $M_{TO}$  and  $M_{LO}$  are dimensionless effective matrix elements connecting  $(1\downarrow)_I$  and  $(0\downarrow)_I$  via the electron-TO- and electron-LO-phonon interaction, respectively.

As can be seen from Fig. 3, where we have plotted  $\mathcal{E}_I$  from (5) very schematically, (5) gives all the pinnings observed in Fig. 2 and requires in addition that the middle branch pin to  $l_2$  from above—a result which is consistent with but not established by our data.<sup>9</sup> The observed absorption strength behavior also seems qualitatively consistent with what we would expect

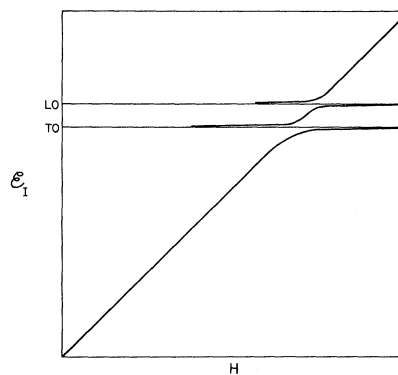


FIG. 3. Schematic plot of pinning behavior of  $\mathcal{E}_I$  expected on the basis of Eq. (5).

from the modified Fröhlich theory.

From the experimental observation that the lower branch absorption seems to die out along  $l_2$  about as fast as the upper branch absorption dies along  $l_3$  we conclude that  $M_{\text{TO}}^2$  is comparable with  $M_{\text{LO}}^2$ ; this last is of order  $\alpha$  from the Fröhlich theory. In InSb  $\alpha \cong 0.02$ .

We do not understand at this time the origin of the unexpectedly strong electron-TO-phonon interaction observed.<sup>10</sup> To get a feeling for how strong this interaction is we substitute for  $f_\mu(k)$  in (4) its value in the conventional deformation potential theory giving<sup>11</sup>

$$f_\mu(k) = \Xi(\hbar/2MN\omega_{\text{TO}})^{1/2}a^{-1}, \quad (6)$$

where we have for convenience simply omitted the angular dependences. In (6)  $N$  is the number of unit cells in the crystal,  $M$  is the reduced mass of In and Sb atoms, and  $a$  is the length of an edge of the unit cell. We find that to make  $M_{\text{TO}}^2$  comparable with  $M_{\text{LO}}^2$  we must take  $\Xi > 100$  eV.

Recent experiments of Onton<sup>12</sup> and co-workers on Si lend indirect support to our conclusion that there exists a reasonably strong electron-TO-phonon interaction in InSb. These experiments seem to demonstrate that optical phonons can interact fairly strongly with electrons by a mechanism not involving lattice polarization. It would be interesting to know whether Onton's  $2p_0$  line exhibits pinning behavior when tuned by calibrated stress or magnetic field.

The existence of electron-TO-phonon interaction in InSb and presumably Si suggests that pinning effects are not confined to polar semiconductors. In particular, such effects should occur in Ge.

If indeed Eq. (4) is the correct generalization of the Fröhlich theory then we would expect to be able to observe free-carrier pinning to  $l_2$  and  $l_3$  from below at "high" temperature. The theory for free-carrier pinning in the Fröhlich model is given in Ref. 4, where it is shown that free carriers should not, however, pin to  $l_3$  or  $l_2$  at low fields. Low-field measurements of the temperature dependence of the absorption indicate that as the donors become ionized the absorption strength for transitions with energy on  $l_3$  diminishes. These results are in at least qualitative agreement with the theory of Ref. 4. "High"-temperature, high-

field measurements are in progress to determine whether free carriers do in fact pin to  $l_2$  and  $l_3$  from below.

Study of the interband transition in which, roughly speaking, electrons are excited from the valence band to the ( $1\uparrow$ ) conduction-band level gives a gap between  $l_2$  and  $l_3$  of  $1.5 \pm 0.2$  meV. While our gap of 1.1 meV seems to be significantly smaller than this, we are not sure at present that the discrepancy is real. Because the determination of a real difference between the gaps would cast new light on the pinning phenomena observed in interband experiments, more precise measurements of the gap would be worthwhile.

We gratefully acknowledge the conscientious efforts of Mr. M. J. Fulton and Mr. P. A. Ligor towards obtaining the highest possible signal-to-noise ratio from our optical system and associated germanium bolometer detector. We also thank Professor A. L. McWhorter and Dr. E. J. Johnson for useful discussions.

\*Visiting Scientist, National Magnet Laboratory, Massachusetts Institute of Technology.

†Operated with support from the U. S. Air Force.

<sup>1</sup>D. H. Dickey, E. J. Johnson, and D. M. Larsen, Phys. Rev. Letters **18**, 599 (1967).

<sup>2</sup>C. J. Summers, P. G. Harper, and S. D. Smith, Solid State Commun. **5**, 615 (1967).

<sup>3</sup>E. J. Johnson and D. M. Larsen, Phys. Rev. Letters **16**, 655 (1966).

<sup>4</sup>D. M. Larsen and E. J. Johnson, J. Phys. Soc. Japan Suppl. **21**, 443 (1966).

<sup>5</sup>B. D. McCombe, S. G. Bishop, and R. Kaplan, Phys. Rev. Letters **18**, 748 (1967).

<sup>6</sup>For a clear discussion of donor impurity levels in InSb in a strong magnetic field see R. F. Wallis and H. J. Bowlden, J. Phys. Chem. Solids **7**, 78 (1958). While we consider it likely that the upper impurity level of our impurity combined resonance transition is in fact ( $1\uparrow$ )<sub>I</sub> defined in the text, the arguments made and conclusion drawn here do not depend upon the correctness of this identification.

<sup>7</sup>M. Haas and B. W. Hennis, J. Phys. Chem. Solids **23**, 1099 (1962).

<sup>8</sup>D. M. Larsen, to be published.

<sup>9</sup>We observe only one low-field absorption which might lie on  $l_2$  and this is at 31 kG and very weak. We were unable to establish a point on  $l_2$  at either 30 or 32 kG, in the first case perhaps because of the expected extreme weakness of the absorption, in the second case perhaps because of the proximity of the tail of the strong absorption on the lower branch, which could have obscured a weak absorption on  $l_2$ .

<sup>10</sup>An argument for why the nonpolar part of the electron-optical-phonon interaction should be very small

in InSb is given on p. 337 of H. Ehrenreich and A. W. Overhauser, Phys. Rev. 104, 331 (1956).

<sup>11</sup>See, for example, R. Loudon, Proc. Roy. Soc. (Lon-

don) A275, 218 (1963).

<sup>12</sup>A. Onton, P. Fisher, and A. K. Ramdas, Phys. Rev. Letters 19, 781 (1967).

### SCHIFF'S PROPOSED GYROSCOPE EXPERIMENT AS A TEST OF THE SCALAR-TENSOR THEORY OF GENERAL RELATIVITY

R. F. O'Connell\*

Institute for Space Studies, Goddard Space Flight Center, National Aeronautics and Space Administration, New York, New York

(Received 20 November 1967)

We compare an explicit expression for the precession of a gyroscope in the Brans-Dicke scalar-tensor general relativity theory with the result derived by Schiff using Einstein's theory, and suggest that the gyroscope experiment offers the best possibility for testing the Brans-Dicke theory. Further, we conclude that the gyroscope in a satellite offers a more sensitive test than the earth-bound gyroscope.

Einstein's general theory of relativity is generally acclaimed as the correct theory of gravitation. Perhaps its only serious challenger is the scalar-tensor theory of Brans-Dicke (BD).<sup>1</sup> In the latter theory the gravitational constant is normalized to give the well-known red-shift result, and the dimensionless coupling constant  $\omega$  is selected to be  $\geq 6$  to ensure that the result for the precession of the perihelion of Mercury agrees, with an accuracy of 8% or less, with the computed value predicted by Einstein's theory. For  $\omega = 6$ , the BD theory gives a precession of 39.6'' arc/century which is about 3.43'' arc/century less than Einstein's value. The recent work of Dicke and Goldenberg<sup>2</sup> on the contribution of solar oblateness to the precession of the perihelion seems to favor the BD theory, but there is considerable controversy surrounding both the measurement itself and the relation<sup>4</sup> between the surface oblateness and the interior oblateness (the latter being the source of the quadrupole moment). It has recently been shown<sup>5</sup> that the rate of gravitational radiation from a system of binary stars in BD theory is smaller than the value predicted by Einstein's theory by a factor of  $(2\omega + 3)/(2\omega + 4)$ ; however, it seems that it will be a considerable time before this test is experimentally feasible. Cosmological tests<sup>6</sup> have likewise been unable to resolve the question. It is our purpose in this communication to suggest that perhaps the best test is the gyroscope experiment proposed by Schiff.<sup>7,8</sup> In particular, we write down an explicit expression for the precession of the gyroscope in BD theory for comparison with the Einstein value.

The angular velocity of precession in Einstein theory,  $\vec{\Omega}_E$  say, may be written as<sup>8</sup>

$$\vec{\Omega}_E = \vec{\Omega}_T + \vec{\Omega}_{DS} + \vec{\Omega}_{LT}, \quad (1)$$

where  $\vec{\Omega}_T$ ,  $\vec{\Omega}_{DS}$  and  $\vec{\Omega}_{LT}$  are the so-called Thomas, de Sitter, and Lense-Thirring contributions, respectively. Explicitly,<sup>8</sup>

$$\Omega_T = \frac{1}{2}(\vec{f} \times \vec{v}), \quad (2a)$$

$$\Omega_{DS} = (3m/2r^3)(\vec{r} \times \vec{v}), \quad (2b)$$

$$\Omega_{LT} = (I/r^3)[(3\vec{r}/r^2)(\vec{\omega} \cdot \vec{r}) - \vec{\omega}], \quad (2c)$$

where  $\vec{f}$  is the acceleration arising from any nongravitational constraint,  $m$  is the mass of the gyroscope ( $c = G = 1$ ),  $\vec{r}$  its position vector with respect to the center of the earth,  $\vec{v}$  is its velocity vector, and  $I$  and  $\omega$  are the moment of inertia and rotational angular velocity of the earth, respectively.

Following Eddington<sup>9</sup> and Robertson<sup>10</sup>, Schiff<sup>11</sup> has written the metric for the nonrotating earth in its most general isotropic form:

$$ds^2 = [1 - 2\alpha(m/r) + 2\beta(m/r)^2 + \dots] dt^2 - [1 + 2\gamma(m/r) + \dots](dx^2 + dy^2 + dz^2), \quad (3)$$

and deduces that the de Sitter term is modified by a factor  $(\alpha + 2\gamma)/3$ . For the particular case of the BD theory it is easy to show that this factor is  $(3\omega + 4)/(3\omega + 6)$ . Being a special-relativistic effect only, the Thomas precession remains unchanged in the BD theory. However, there is a change in the Lense-Thirring effect which is deduced quite easily from an observation made by the present author and